Towards Quantitative Wall Shear Stress Measurements: Considering the Flow Behavior of Liquid Crystals

Stefanos Melekidis, Marcus Ebert*, Jonas Schmid, Hans-Jörg Bauer
stefanos.melekidis@kit.edu

Institute of Thermal Turbomachinery (ITS),
Karlsruhe Institute of Technology (KIT),
Kaiserstrasse 12, 76131 Karlsruhe,
Germany

Abstract

Liquid crystal diagnostics is a suitable tool for determining quantitative wall shear stress distributions with high spatial resolution, which may be applied to almost any surface shape. To determine a wall shear stress vector field, the state-of-the-art calibration procedure requires taking multiple images of the liquid crystal-coated surface from different points of view. In literature, it is reported that this data acquisition is usually performed using several, up to six, commercially available consumer cameras to synchronously record the liquid crystal signal. However, the need for several recording devices makes measurement diagnostics unsuitable even for laboratory measurements, as often only one camera of identical construction is available. Using a single camera produces a different wall shear stress vector field due to the time-dependent liquid crystal signal, which results from the time offset between the individual exposures compared to the synchronous exposures under otherwise identical boundary conditions. This time dependence follows from the thixotropic behavior of the liquid crystals. In addition, two other effects, one of which is not described in literature, affect the liquid crystal color signal. In order to record physical and reliable data with a single camera, it is essential to record images only when the liquid crystal signal is quasi-stationary.

The main objective of this paper is to provide recommendations for the acquisition of liquid crystal data using a single camera. In a first step, a start time is defined, from which quasi-stationary liquid crystal data can be acquired experimentally within a certain time interval. A flat plate wind tunnel is used for this purpose. The specified time constraints are valid for measurements, in which liquid crystal mixtures with a viscosity $\leq$ 750...1 250 mPa s are used, e. g. BCN/192 from LCRHallcrest Ltd., at a maximum wall shear stress of $\leq$ 34 Pa. Using the derived time constraints, the error with respect to the wall shear stress magnitude and its direction can be reduced. The concluding discussion may serve as a guideline for reliable liquid crystal data acquisition to make the measurement technique applicable in practice even when a single camera is available only.

Keywords: Liquid crystals; wall shear stress; flow behavior; thixotropy; temperature dependence; hue calibration; experimental data; commercial consumer camera; subsonic flow; quasi-stationary measurement; temperature scaling approach

* Is no longer at Karlsruhe Institute of Technology.

Nomenclature

Latin

C	[K]	Sutherland constant
H	[°]	Hue
H_τ	[°]	Relative wall shear stress or vector-aligned hue (H at ϕ_τ)
L_{char}	[m]	Characteristic length
R	[Jkg^{-1}K^{-1}]	Specific gas constant
$\{R, G, B\}$	[A.U.]	Red, green, and blue detector signal in sRGB color space
T	[K]	Temperature
T_0	[K]	Sutherland reference temperature
a	[ms^{-1}]	Speed of sound
$\{a, b, c, d\}$	[−]	Fit function coefficients
c_f	[−]	Skin friction coefficient
j	[−]	Exponent
k	[−]	Aperture value
m	[−]	Arbitrary constant (slope)
m	[−]	Number of circumferential positions
n	[−]	Number of images for averaging
p	[m]	Pitch of helix structure
$\dot{q}$	[Wm^{-2}]	Specific heat flux
t	[s]	Time
t_{acq}	[s]	Liquid crystal data acquisition time interval
t_{pre}	[s]	Liquid crystal coating pre-load time
u	[ms^{-1}]	Streamwise velocity
x	[m]	Streamwise coordinate
y	[m]	Wall-normal coordinate
z	[m]	Lateral coordinate

Greek

α	[Wm^{-2}K^{-1}]	Heat transfer coefficient
α_c	[°]	Above-plane viewing angle (polar)
κ	[−]	Isentropic exponent
κ	[−]	Karman constant
λ	[m]	Dominant wavelength
λ	[Wm^{-1}K^{-1}]	Thermal conductivity
μ	[Pas]	Dynamic viscosity
μ_0	[Pas]	Sutherland reference dynamic viscosity
ρ	[kgm^{-3}]	Density
τ	[Pa]	Wall shear stress magnitude
ϕ_τ	[°]	Angle at vector-aligned hue (ϕ at H_τ)
ϕ_c	[°]	Circumferential viewing angle (azimuthal)

Scripts

$\square_1$	First state
$\square_2$	Second state
$\square_\text{i}$	Running index
$\square_\text{ref}$	Reference
$\square_\text{s}$	Solid

Similarity parameters

$\mathrm{Bi} = \frac{\alpha L_{\mathrm{char}}}{\lambda_{\mathrm{s}}}$	Biot number
$\mathrm{Ma} = \frac{u}{a} = \frac{u}{\sqrt{\kappa R T}}$	Mach number
$\mathrm{Re} = \frac{u \rho L_{\mathrm{char}}}{\mu}$	Reynolds number
$\mathrm{Tu} = C \left(\frac{x}{d} \right)^{-5/7}$	Free-stream turbulence intensity according to Roach [1]

Abbreviations

FMR	Fluid mechanics-related
ISO	International Organization for Standardization
KIT	Karlsruhe Institute of Technology
LC	Liquid crystals
LCR	Liquid crystal-related
sRGB	Standard RGB (red, green, blue) color space

1.0 TOWARDS QUANTITATIVE WALL SHEAR STRESS MEASUREMENTS USING A SINGLE CAMERA

Liquid crystal diagnostics can be used to determine locally resolved wall shear stress vector fields in many engineering applications. Its main alternatives are conventional methods, such as mechanical float balances, Preston tubes, hot-wire anemometry, or hot-film measuring devices that may provide accurate and partly high-frequency data. However, such sensors only cover the area-averaged target value or provide local information at specific points on a surface. Furthermore, their intrusive use may significantly affect flow. More importantly, the spatial resolution of conventional sensors is inherently limited by the dimensions of the sensor. Consequently, determining a high-resolution two-dimensional wall shear stress distribution on an arbitrarily shaped surface requires the use of numerous sensors, each of which has to be attached to the target surface. This, however, is often not feasible, can be time-consuming and costly, and disturbs the boundary layer even more. In addition, such sensors interfere with each other, if they are mounted too close to each other. In such a case, liquid crystal measurement technology has clear advantages. In particular, it is non-intrusive and has a high spatial resolution.

Reda and Muratore [2] also recognized the potential. They were the first to describe a quantitative measurement technique to determine wall shear stress distributions using liquid crystals. During their investigations, they found that the color response of liquid crystals depends on both the wall shear stress magnitude and its direction. For data acquisition, they used spectroscopy (wavelength, point data) and photogrammetry (RGB and hue, respectively, two-dimensional data) and showed that wall shear stress vector fields can be determined using both quantities. To determine the wall shear stress distribution, a camera was utilized to acquire images of the liquid crystal-coated surface from different viewing angles around the region of interest. In an early study [3], Reda et al. stated that the response time of liquid crystals is in the order of milliseconds and that a liquid crystal coating may be exposed to multiple loads. In later publications, they used a new liquid crystal coating for each viewing angle, from which they recorded the data during the measurement, but did not give the reasons.

Fujisawa et al. [4] investigated a flow around a cylinder using an approach other than described in the measurement procedure by Reda and Muratore [2]. They used two cameras with a constant illumination angle, symmetrically aligned with respect to the flow direction.

Zhao et al. [5] used multiple identical cameras in their measurements to synchronously record data of the shear-sensitive, temperature-insensitive liquid crystal-coated region of interest. From this data, they derived the wall shear stress direction. To determine the magnitude, they created a calibration curve by approaching several operating points. For each operating point, they used a newly coated measurement insert. Zhao et al. [5] were first to report qualitative observations regarding the time behavior of liquid crystals and stated that more research is required. Based on their findings, subsequent measurements were conducted after pre-loading the liquid crystal coating for $\approx 100\,\mathrm{s}$. However, this value was derived at a velocity of $27.4\,\mathrm{ms}^{-1}$, which may not be representative

of studies at supersonic velocities, see Zhao [6]. Their investigations covered symmetric flows, specifically a (supersonic) free jet flow [5–9].

The current state of literature on the applicability and use of liquid crystal diagnostics can be characterized as follows:

- Limited to symmetrical (simple) flows,
- highly individual situation and requirements of recording, e. g. case-specific experimental setup,
- highly individual approach with regard to the measurement procedure, e. g. number/change of liquid crystal-coated measurement inserts,
- no information on specific temporal boundary conditions of recording,
- no universally valid, established calibration database, and
- liquid crystal mixtures for wall shear stress measurements are described as being temperature-insensitive, which has not yet been verified.

The different approaches regarding the usage of liquid crystals in conjunction with a hysteresis of their color response to multiple exposures reported by Anderson and Baughn [10] suggest that there is a lack of knowledge on liquid crystal data acquisition which renders the diagnostics not robust and error-prone. Furthermore, it is evident that the need for several acquisition devices makes the measurement technique impractical. To fill this research gap regarding data acquisition and make it reasonably applicable using a single consumer camera, the time response of the liquid crystal color signal is investigated. From experimental time recordings, a physical start time and a measurement interval are derived, from which and within which the liquid crystal signal is quasi-stationary. In this way, guidelines for liquid crystal measurements with a single camera are established. Furthermore, it is shown that liquid crystal imaging without considering such criteria leads to non-physical wall shear stress vector fields. Finally, the effects of time constrains on the resulting wall shear stress vector field are discussed. For the discussion, the necessary liquid crystal fundamentals, the experimental flat plate setup, and the measurement principle are presented and explained in more detail.

2.0 LIQUID CRYSTAL DIAGNOSTICS AND EXPERIMENTAL SETUP

Liquid crystals[†] selectively scatter incident light of the visible spectrum. This is due to their properties, namely, birefringence, circular dichroism, and the characteristic length, the pitch p. It is in the order of magnitude of the wavelength λ of visible light, $\lambda \approx p$. With varying pitch of the helical structure, selective scattering of incident light changes. For the liquid crystal mixtures used, this helix pitch depends mainly on the wall shear stresses and only to a limited extent on temperature and pressure. This results in the relation

$$p \propto \lambda \propto \tau^{-j} \quad \text{with } j > 0, \tag{1}$$

between the pitch, the wavelength of the scattered light, and the wall shear stress τ, with j being an exponent larger than zero. Consequently, an increase in wall shear stress is related to a shorter wavelength of the selectively scattered light resulting from a decrease in helical pitch. This change in wavelength is used for determining wall shear stresses by means of liquid crystal diagnostics.

An ordered alignment of the optical axis of the helical structure is a prerequisite for using the relation given in Eq. 1. The alignment of the liquid crystal molecules from a disordered to an ordered structure can be achieved, e. g., by shearing the liquid crystal coating using a stream of compressed air over the coating or by fine brushing. The three states relevant to measuring wall shear stresses are illustrated in Fig. 1.

In the focal-conic state, see Fig. 1a, the axes of the helices are disordered and at a low energy level. In this state, the liquid crystal texture is birefringent, but optically semi-active, such that incident light is only randomly and not selectively scattered in the classical physical sense. A certain color may be perceived in the optically active planar or Grandjean texture of the liquid crystal layer, see Fig. 1b. The color results from the ordered helical axes which are orthogonal to the coated surface. However, no selective scattering of light takes place at this point. From Fig. 1c, it is obvious that a tilting of the helical axes due to the flow-induced shear forces along the surface occurs in addition to the change in helical pitch due to temperature changes. This means that two effects are superimposed: The scattering of light due to the change in pitch of the chiral-nematic liquid crystal planes and selective scattering of light due to the tilting of the helical axes under load. This is the primary feature

[†] In the following sections, the optically active chiral-nematic phase is referred to exclusively. More information on the light propagation in liquid crystals is given in [11].

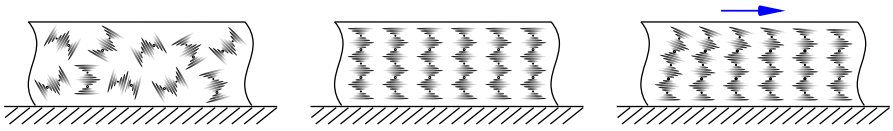

(a) Focal-conic state (b) Planar state (unloaded) (c) Planar state (loaded)

Figure 1: Structures of chiral-nematic liquid crystal coatings for wall shear stress measurements: Molecules before (Fig. 1a) and after alignment (Fig. 1b) as well as during load (Fig. 1c) according to Bonnett [12] adapted from Melekidis et al. [11]. The flow direction is illustrated by the blue arrow.

that allows wall shear stresses to be visualized using liquid crystals and subsequently quantified using a suitable calibration.

To determine wall shear stress, a substitute quantity, hue H is described and used in literature instead of the wavelength [13]. In the context of liquid crystal measurement technology, hue is used as a measure of physical wavelength that is decoupled from light intensity. Reda and Muratore [2] and Reda et al. [13] carried out liquid crystal measurements using a spectrometer (wavelength, point data) and a camera (RGB and hue, respectively, two-dimensional data) and demonstrated that wall shear stress vector fields can be determined using both quantities. The relation between the wavelength and hue is $\lambda \propto mH^{-1}$, with m being a constant affecting the slope. Based on their findings, they formulated a hue-based approach [2] which is also used in this paper to determine wall shear stress vector fields.

The selectively scattered light is typically acquired using a standard consumer camera. After further processing of the intensity values (debayering/demosaicing), the liquid crystal signal may be in the form of red, green, and blue values (RGB) in the standard RGB ($sRGB$) color space using the RGB color model. It is then converted to the hue. For this, the conversion algorithm by Bajon et al. [14] is used. With the transformed quantity, the hue-based approach according to Reda and Muratore [2] can be utilized. More information on the relation between wavelength, RGB, hue, and the conversion algorithm used, can be found in the study by Melekidis et al. [11].

Reda and Muratore [2] observed in their investigations that the hue changes under load depending on the observation angle. For the observation angle, they considered an azimuth ϕ_c and a polar angle α_c. The resulting three-dimensional color spectrum under load can be illustrated as a function of the illumination angle chosen orthogonally to the region of interest and the introduced observation angles relative to the aligned liquid crystal layer as a function of local wall shear stress, see Fig. 2. The position of an observer in the xz-plane of the liquid

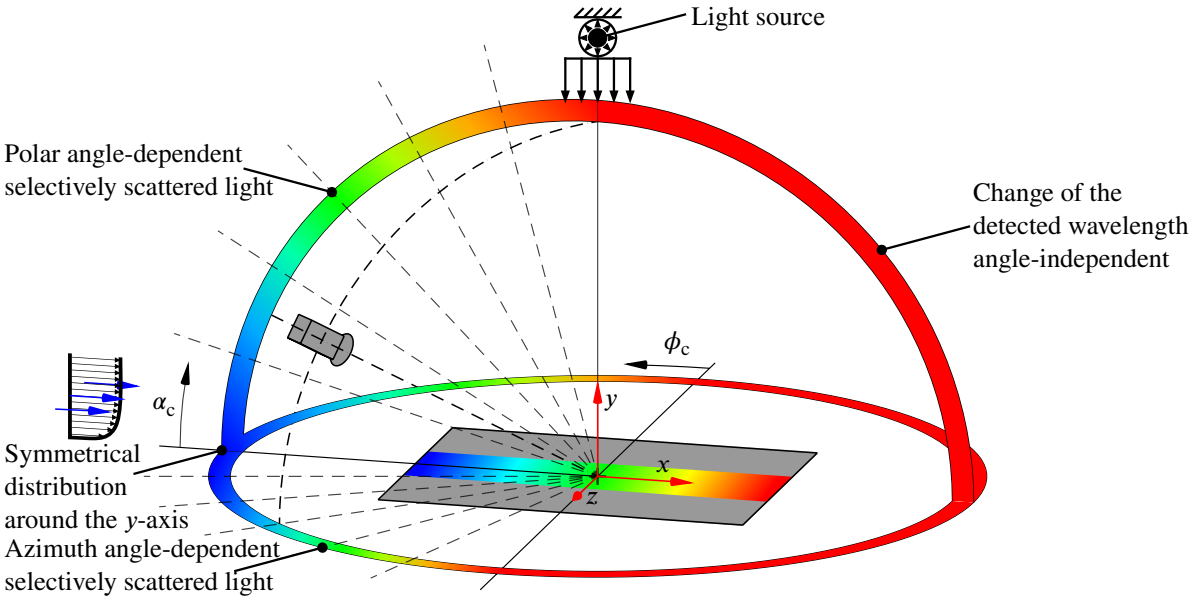

Figure 2: Selectively scattered light, displayed as colors, as a function of azimuth angle ϕ_c and polar angle α_c, illustrated schematically for steady-state flow along a flat plate. The blue arrows are representative of the flow direction with a turbulent velocity profile in between from Melekidis et al. [11].

crystal surface is described by the azimuth angle. In contrast to this, the inclination of an observer relative to this plane is given by the polar angle. Based on their measurements, Reda and Muratore concluded that the minimum

dominant wavelength is measured when the direction of the wall shear stress vector is congruent with the direction of observation and points away from the observer. This angle-dependent selective scattering of light occurs only when the liquid crystals are loaded. This may be achieved by an air flow along a flat plate and is represented by a turbulent velocity profile in Fig. 2. The flow direction corresponds to the x-direction and is illustrated by the blue arrows.

For liquid crystal measurements, the geometrical relations between observer, illumination, and region of interest illustrated in Fig. 2 have to be taken into account as well as the requirements of the hue-based approach by Reda and Muratore [2]. Moreover, to further develop liquid crystal diagnostics, well-known boundary conditions are needed for the experimental setup. For these reasons, the Liquid Crystal Test Rig, consisting of a wind tunnel equipped with a generic flat plate test section that fully meets these requirements, was designed and built at the Institute of Thermal Turbomachinery at Karlsruhe Institute of Technology (KIT), see Fig. 3. In the following sections, only the new features of the experimental setup, see [15], within the test section and their implications on calculated or measured quantities are discussed.

The updated test section is displayed schematically in Fig. 3. All circled numbers refer to this schematic representation. In order to increase the maximum wall shear stress investigated, a new, more powerful blower is used

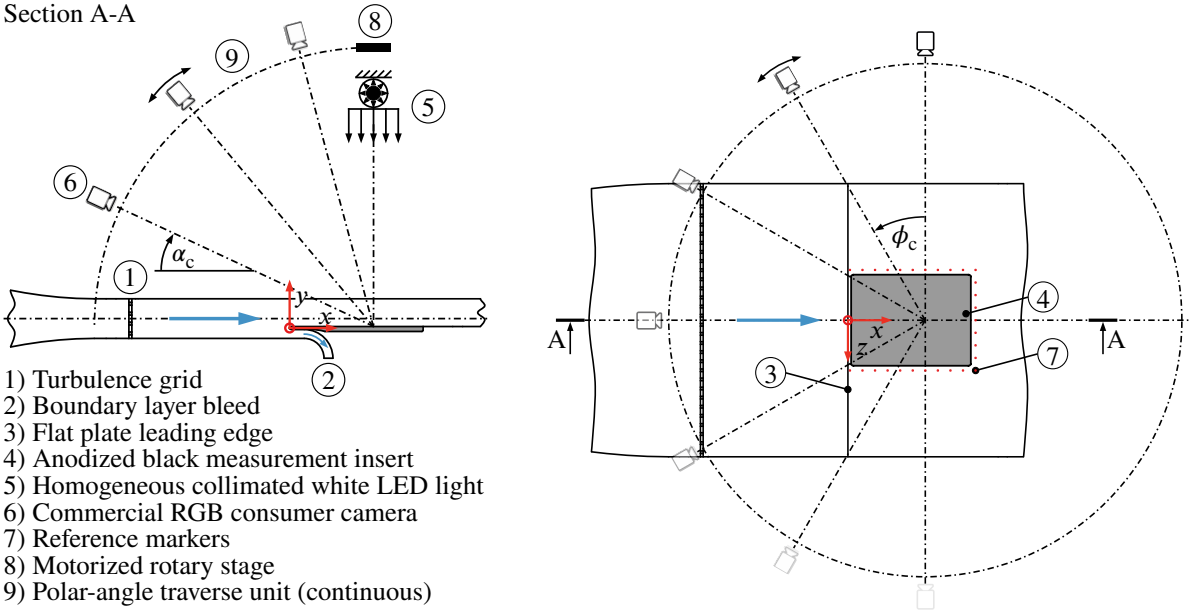

1) Turbulence grid
2) Boundary layer bleed
3) Flat plate leading edge
4) Anodized black measurement insert
5) Homogeneous collimated white LED light
6) Commercial RGB consumer camera
7) Reference markers
8) Motorized rotary stage
9) Polar-angle traverse unit (continuous)

(a) Side view

(b) Top view (without illumination and motorized rotary stage)

Figure 3: Updated test section, including a sketch of the camera traverse and the illumination setup adapted from Melekidis et al. [15].

and the measurement insert ④ to which the liquid crystals are applied is extended in the upstream direction. Due to this extension from 100 mm to 131 mm, the measuring range also covers a region of a higher wall shear stress as a result of the lower boundary layer height and the related steeper velocity gradient. Using the Schlichting correlation [16], the range obtained in this way is calculated to be approximately 11 Pa. This measure is accompanied by a change in the free stream turbulence intensity designed in [15]. It is now Tu = 6.40 % instead of 5.65 % with respect to the new measurement insert leading edge ③.

To obtain reproducible data, repeatable positioning of the camera relative to the measurement insert is required. For the azimuthal alignment, see ϕ_c in Fig. 3b, this is achieved by a motorized rotary stage ⑧ with a repeatability of 0.01°. The polar angle between the camera and the measurement insert, see α_c in Fig. 3a, can be continuously adjusted via the designed polar-angle traverse unit ⑨, which consists of a lockable tongue and groove joint. These measures guarantee a wide range of well-adjustable observation angles.

Using the displayed Liquid Crystal Test Rig, measurable boundary conditions are obtained. Both operating point stability and velocity and temperature profiles were investigated [15], showing outstanding operating point stability over time and desired aerothermal profiles, thus offering the possibility to use analytical correlations for the determination of wall shear stresses in a first step as a calibration reference.

In addition to these boundary conditions, it is crucial to operate the test rig at Reynolds similarity, since flows are then similar regardless of their geometry. This is an essential prerequisite for the subsequent transferability of

the wall shear stress measurements and the newly gained knowledge to technically closer geometries. A pneumatic high-frequency control valve compensates the decreasing Reynolds number due to the increasing air temperature during a measurement. This temperature increase results from the heating in the multistage centrifugal blower and the infrastructure. More precisely, by opening the valve, the pressure drop is reduced and the front pressure is increased, causing the mass flow and consequently the velocity to increase. This approach allows the Reynolds number and thus the operating point to be kept constant in the event of temperature changes.

3.0 EVALUATION APPROACHES AND METHODOLOGY

For liquid crystal signal acquisition, new challenges result from the described heating of the process air and, hence, of the test rig, while they are stressed by a flow, i.e. are in a planar loaded state, see Fig. 1c. In addition, liquid crystals exhibit an effect even in the unloaded focal-conic state, see Fig. 1a, e. g. when the substrate to which they are applied is heated, which changes the material values of the liquid crystals. The emerging effects are divided into liquid crystal-related (LCR) and fluid mechanics-related (FMR) phenomena and are shown in Fig. 4 for better understanding. The first phenomenon is referred to as thixotropy in rheology (LCR-I), see Fig. 4a, and

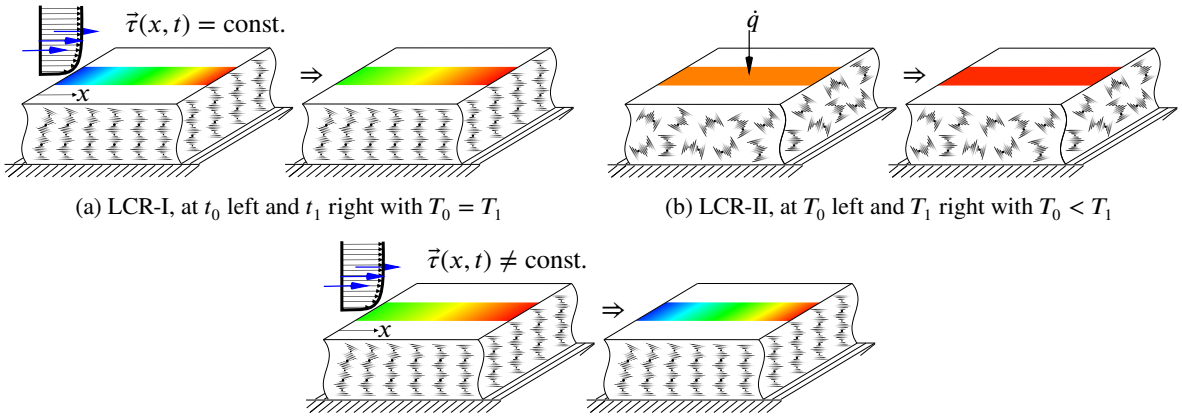

(a) LCR-I, at t_0 left and t_1 right with $T_0 = T_1$

(b) LCR-II, at T_0 left and T_1 right with $T_0 < T_1$

(c) FMR, at T_0 left and T_1 right with $T_0 < T_1$

Figure 4: Impact of the three effects on the liquid crystal color signal acquired during a measurement due to the sustained stress on the liquid crystal layer and due to the temperature increase caused by the test facility. The latter causes both a heating of the liquid crystal layer and an increase in wall shear stress due to the temperature-induced increase in viscosity.

describes a time dependence of the flow properties in non-Newtonian fluids. Liquid crystals used to determine wall shear stresses are non-Newtonian [17], which is why their viscosity decreases as a result of continuous external forces and stresses, respectively. The decreasing viscosity comes along with a change in the liquid crystal color signal. Furthermore, the wall shear stresses at the respective x-position are constant over time, see Fig. 4a. The second phenomenon is a temperature-related effect, namely, the decrease in liquid crystal viscosity due to an increase in liquid crystal temperature (LCR-II), see Fig. 4b, which is reflected by the specific heat flux $\dot{q}$. Even in this case, a change in the liquid crystal signal can be observed, namely, the decrease of the hue with increasing temperature. The latter effect results from the increase in wall shear stress and air viscosity, respectively, as a result of the increase in temperature over time during a measurement assuming Reynolds similarity (FMR), see Fig. 4c, and consequently is not constant contrary to (LCR-I). This, in turn, is related to a shorter wavelength of the selectively scattered light, i. e. a higher hue value, resulting from a decrease in helical pitch, see Eq. 1. All the above effects lead to a change in the liquid crystal color signal and are superimposed on each other. In the following section, concepts for the different effects are presented which, to the authors' knowledge, have not yet been reported in literature in this form. Two of the three approaches presented, for (LCR-I) and (FMR), are also used for the final data collection and its subsequent evaluation. Note that the approach derived for (FMR) is a prerequisite for deriving an approach to effect (LCR-I).

3.1 Reflections on the Phenomena

To counteract (FMR), the general relation

$$\tau = \frac{1}{2}\rho {u_x}^2 c_\mathrm{f}, \tag{2}$$

between wall shear stress, density of the fluid ρ, flow velocity u_x, and skin friction coefficient c_f is used. The skin friction coefficient may be replaced by the empirical correlation of Schlichting et al. [16]

$$c_f = 2\left[\frac{\kappa}{\ln(\mathrm{Re}_x)}G(\ln(\mathrm{Re}_x))\right]^2, \tag{3}$$

which is also used in this work. There, κ is the Karman constant equal to 0.41, $G(\ln(\mathrm{Re}_x))$ is a function dependent on $\ln(\mathrm{Re}_x)$ and takes the value $G(\ln(\mathrm{Re}_x)) \approx 1.5$ within the Reynolds number range of $10^5 < \mathrm{Re}_x < 10^6$. From Eq. 2 it follows that the density and, hence, the velocity change with increasing temperature, which affects the wall shear stress linearly (density) or quadratically (velocity) and makes scaling of the wall shear stress reasonable. For the scaling, the reference values from Table 1 are used. Assuming Reynolds similarity and using Eq. 2 in

Table 1: Reference flow parameters for evaluation. The quantities refer to the leading edge of the measuring insert, which is 4 mm downstream of the leading edge of the flat plate, where the coordinate system origin is also defined, see Fig. 3.

Quantity	Value
Reference temperature T_{ref}	305.0 K
Streamwise velocity u	89.0 ms^{-1}
Reynolds number Re	34 440
Wall shear stress magnitude τ	33.1 Pa

combination with

$$\mathrm{Re} = \frac{u\rho L_{\mathrm{char}}}{\mu} \text{ and } \mu = \mu_0 \frac{T_0 + C}{T + C}\left(\frac{T}{T_0}\right)^{\frac{3}{2}}, \tag{4}$$

leads to the generally valid relation

$$\frac{\tau_2}{\tau_{1,\mathrm{ref}}} = \frac{\rho_{1,\mathrm{ref}}}{\rho_2}\left(\frac{T_{1,\mathrm{ref}} + C}{T_2 + C}\right)^2\left(\frac{T_2}{T_{1,\mathrm{ref}}}\right)^3, \tag{5}$$

between the wall shear stress, density, temperature, and the Sutherland constant. The Reynolds number Re consists of the flow velocity, the density, the characteristic length at the position $L_{\mathrm{char}} = x$ and the dynamic viscosity μ. The latter is calculated using the Sutherland model [18] with the reference dynamic viscosity $\mu_0 = 17.16 \times 10^{-6}$ Pa s, Sutherland constant $C = 111$ K, reference temperature $T_0 = 273$ K, and temperature T. The latter is measured by means of a Class 1, type K (nickel-chromium-nickel) thermocouple located downstream of the liquid crystal measuring insert inside the reference probe used to set the operating point, see [15]. In this case, temperature T_2 corresponds to the air temperature of the free flow. Considering the boundaries of the experimental setup, Eq. 5 may be simplified. It is assumed that the pressure change after the correct setting of an operating point is negligible. Furthermore, the density changes only slightly within the temperature range $T = 293...310$ K and the test rig operates at approximately atmospheric pressure. This is also supported by the argumentation based on the Mach number Ma, for which, as long as it is in the subsonic regime, compressibility effects may be neglected. Based on measured data, the density change in the specified temperature range is calculated to be $\approx 4\,\%$. This finally leads to

$$\frac{\tau_2}{\tau_{1,\mathrm{ref}}} = \left(\frac{T_{1,\mathrm{ref}} + C}{T_2 + C}\right)^2\left(\frac{T_2}{T_{1,\mathrm{ref}}}\right)^3. \tag{6}$$

With the described scaling approach and the test rig, see Section 2, the liquid crystal data are comparable at different fluid temperatures and, hence, different wall shear stresses, see (FMR). To ensure this comparability, it is essential to always record the data at the same illumination and recording device settings. The requirements are listed in Table A1, see Appendix A, and are representative during a measurement.

To investigate the effect (LCR-II), the substrate to which the liquid crystals are applied is heated in a controlled manner. Heating takes place in the absence of an air flow along the liquid crystals. To determine the liquid crystal signal-temperature relation in the unloaded, focal-conic state, see Fig. 1a, a 5 mm thick copper plate is placed underneath the liquid crystal measurement insert with thermal paste in between. An electrical heating element on the back of the plate heats the copper material and thereby the measurement insert to which the liquid crystals are applied. The temperature increase is approximately $\frac{\Delta T}{\Delta t} \approx 0.01$ Ks^{-1}. The influence of free

convection is negligible due to the small temperature differences from the environment and the resulting small density differences in the ambient air. The Biot number Bi is estimated for the present case and is several orders of magnitude below the critical Biot number. This fact, in combination with the slow heating of the liquid crystals, allows the internal temperature gradients to be neglected. The temperature characteristic over time is recorded using a thermocouple on the substrate underneath the liquid crystal layer. During heating, an image is automatically taken every 30 s. The color signal recorded at a specific above-plane viewing angle is then transformed using the conversion algorithm according to Bajon et al. [14] and averaged at the center of the measurement insert over a pixel range $z \times x = 50\,\text{px} \times 50\,\text{px}$. The decreasing hue characteristic over temperature is exponential for the relevant temperature range and amounts to $\approx 10°$. This decrease in hue can be approximated by a two-term exponential function with coefficients $a = 565.6$, $b = -0.2086$, $c = 32.32$, and $d = -0.01579$. At the specified temperature range, the thermal expansion of the aluminum measurement insert is in the single-digit hundredths of a millimeter range, which allows the thermal expansion of the substrate and the associated stresses in the liquid crystal coating to be neglected.

3.2 Hue-based Approach

Liquid crystal data is analyzed using the calibration method proposed by Reda and Muratore [2], which allows wall shear stresses to be quantified in both magnitude and direction. This is described and illustrated in Fig. 5. According to steps **I** to **IV**, the vector field can be calculated by calibrating the detected liquid crystal signal in

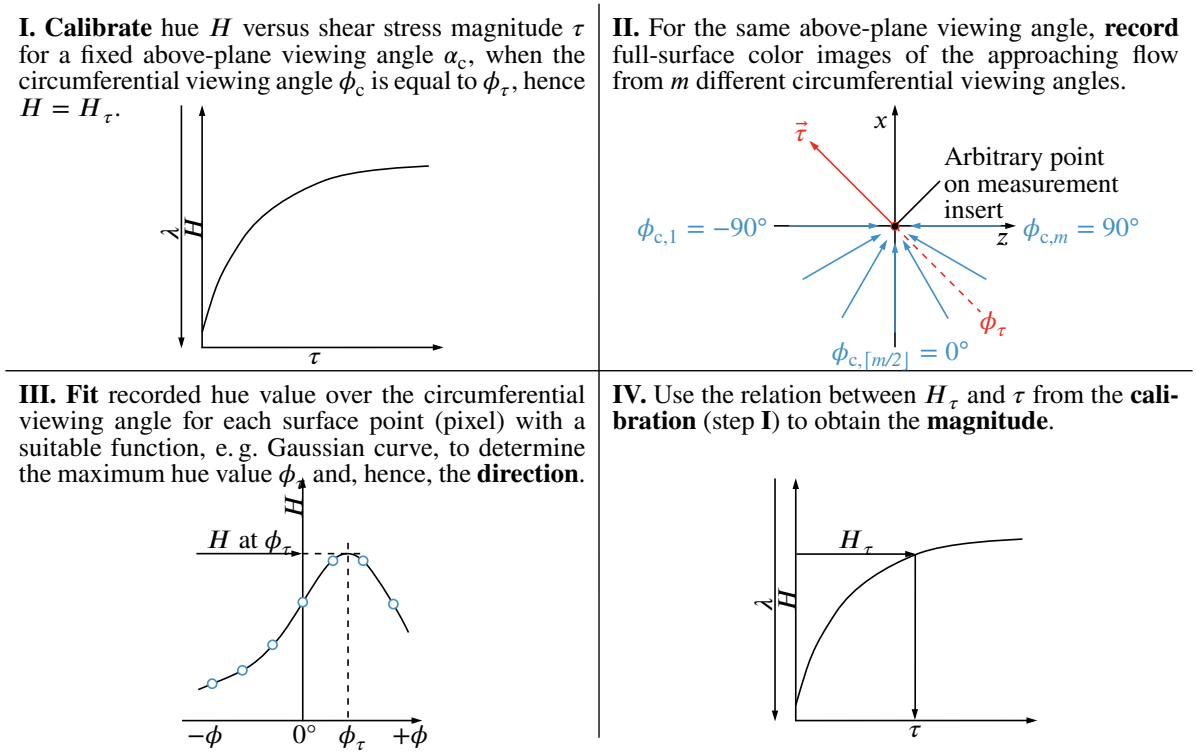

Figure 5: Diagnostic principle for measuring wall shear stress vector fields, according to Reda and Muratore [2] adapted by Zhao [6] and Melekidis et al. [15].

the direction of the wall shear stress vector with respect to the prevailing local wall shear stress magnitude.

It is now assumed that both the illumination and camera settings and the polar angle remain unchanged throughout the experiment. This is ensured by the experimental setup, see Fig. 3. In step **I**, see Fig. 5, the color response of the liquid crystals is recorded at a known magnitude and direction of the wall shear stress at a fixed polar angle α_c, referred to as above-plane viewing angle. The minimum dominant wavelength λ_{min}, i.e., the maximum color change and, hence, the maximum wall shear stress occurs at α_c where the shear vector is aligned with and directed away from the observer. This angular orientation defines the vector orientation ϕ_τ and is therefore referred to as the angle at vector-aligned hue. For a given setup and fixed above-plane viewing angle, the acquired RGB values at the respective azimuth angle depend exclusively on the locally induced wall shear stress magnitude and no longer on its direction. Using one of the alternative measurement techniques mentioned in Section 1, an in-situ

calibration can be performed to assign the recorded color signal to the local wall shear stress. For the subsequent evaluation of the experimental liquid crystal data presented in this paper, the correlation by Schlichting [16] is used, see Eq. 3. Based on this correlation, the magnitude of the wall shear stress is quantified, see step **I** in Fig. 5.

In step **II** to determine the wall shear stress vector field of an unknown flow, a number of n images are acquired at each azimuth angle ϕ_c, referred to as circumferential viewing angle. The images are acquired between $-90° \leq \phi_c \leq 90°$ at m circumferential positions at constant above-plane viewing angle.

In step **III**, the color values of the number of images transformed with the conversion algorithm by Bajon et al. [14], see [11], are approximated using a Gaussian distribution. The maximum of the fitted distribution corresponds to the angle of the local wall shear stress direction and is referred to as vector-aligned hue.

In step **IV**, the magnitude of the local wall shear stress is determined from the maximum of the Gaussian distribution (H_τ) corresponding to the minimum dominant wavelength and, thus, the maximum hue value using the calibration curve from step **I**, see Fig. 5.

Steps **III** and **IV** are repeated for each image point (pixel) in the region of interest to obtain a complete quantitative two-dimensional wall shear stress vector field.

In summary, it can be seen in particular from steps **II** and **III** that multiple recordings are necessary to calculate the wall shear stress direction and, via H_τ, the wall shear stress magnitude of an unknown flow. To date, the images have often been recorded with many identical cameras, which renders the measurement technique impractical. The more practical measurement diagnosis with a single camera shows the flow behavior of the liquid crystals due to the time offset between the images and the temperature increase during a measurement. This flow behavior, if not taken into account, leads to non-physical wall shear stress distributions. Consequently, the created calibration curve, see step **I**, may not be valid, unless appropriate measures are taken.

Furthermore, the liquid crystal mixtures produced by LCRHallcrest Ltd., e. g. BCN/192, CN/R3, and CN/R2, are described by the manufacturer and in literature as shear-sensitive (temperature-insensitive) liquid crystals. However, even in the unloaded, focal-conical state, they show a decrease in hue with an increase in temperature when no flow is apparent. This effect, in combination with the flow behavior observed by single-camera imaging, leads to a coupling of shear stress- and temperature-induced flow of the liquid crystal coating, resulting in a significant change in hue. As a countermeasure, time constraints are determined experimentally and recommendations are given for liquid crystal diagnostics using a single camera in the next section.

4.0 RESULTS AND DISCUSSION

The derived wall shear stress scaling approach, see Eq. 6, is used to correct the wall shear stress at each acquisition time. This is a prerequisite for the development of an approach to account for the effect (LCR-I). From Fig. 6 it follows that as the runtime increases, i. e. with increasing air temperature, the hue value decreases beyond a certain limit for the same wall shear stress. This limit is illustrated by the vertical line and the arrow pointing in the direction of values $\lessapprox 31$ Pa. The values left of the inflection point cannot be explained on the basis of the data available. The change from positive to negative differences $\Delta H = H_{t_1} - H_{t_0}$ between the respective time steps may be due to the stripping of the liquid crystal coating over time and the related difference in its absorption/reflection behavior. To illustrate the influence of scaling, the start and end positions of the liquid crystal measurement insert are shown on the second abscissa, with the start points (green) and end points (red). These points are shifted horizontally towards higher wall shear stresses, i. e. to the left along the abscissa, due to the wall shear stress scaling for the individual curves, see Eq. 6. Furthermore, no steady-state hue characteristic develops even after long measuring times. This results in the requirement of a pre-load time t_{pre} for the liquid crystal coating, after which the hue change does not drop below a certain value within a defined data acquisition time interval t_{acq}.

For this purpose, a tolerable threshold and a minimum recording time have to be specified. The threshold is set to e. g. $\Delta H = -2°$. The data acquisition time interval, in which this deviation of hue over time is allowed, is set to e. g. $t_{acq} = 300$ s. It results from the requirements for a liquid crystal measurement of an unknown flow, see step **II** in Fig. 5. Such a measurement is based on two camera round trips around the test section from $\phi_c = -90°$ to $\phi_c = 90°$ and back, a change of the above-plane viewing angle which lasts ≈ 20 s, $n = 1$ camera recordings at $m = 11$ azimuthal positions, with one round trip lasting ≈ 140 s.

‡ Note that the wall shear stress decreases with $\frac{1}{\ln(x)^2}$ using the Schlichting correlation [16], which is why the geometric center is not in the middle of the abscissa, but clearly right of it, see the red box.

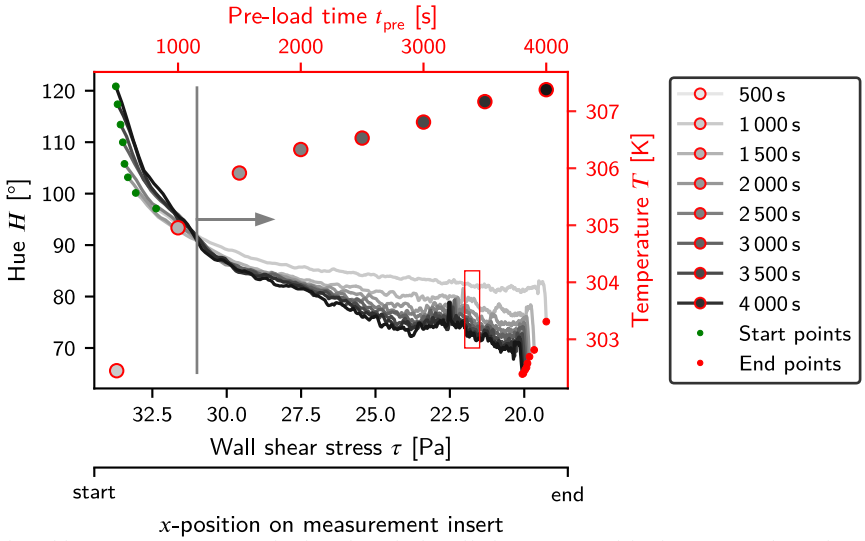

Figure 6: Calculated hue average versus the local scaled wall shear stress (black axes) and pre-load time versus air temperature (red axes) at different pre-load times, displayed every 500 s. The circles outlined in red belong to the red axes and are shown in the legend according to their pre-load time. The red box represents the data evaluation interval, which is distributed around the scaled wall shear stress at a reference temperature of $T_{ref} = 305$ K in the optical center[‡] of the measurement insert. The hue data results from the three effects described in Section 3.

From the defined threshold as well as the selected time interval, a corresponding pre-load time may be determined using

$$\Delta H_i = \frac{\Delta H}{\frac{t_{acq}}{\Delta t_i}}. \tag{7}$$

In contrast to the liquid crystal measurement described in Fig. 5, only images from $\phi_c = 0°$ are taken for this purpose. At this position, the vector-aligned hue H_τ can be recorded. Here, once again, it is important to precisely know the flow and its direction, which is why the Liquid Crystal Test Rig at the Institute of Thermal Turbomachinery at KIT is a key element for quantitative wall shear stress measurements using liquid crystal diagnostics. The vector-aligned hue is acquired automatically every $\Delta t_i = 100$ s over a period of 4 000 s at a fixed above-plane viewing angle. Due to the temperature increase during a measurement described in Section 2, the viscosity increases, which leads to an increase in the wall shear stress which makes the scaling approach introduced in Eq. 6 indispensable. This approach accounts for the fact that despite the increasing air temperature, only hue values at the same wall shear stress are used for evaluation, see Fig. 4c, thus making hue values comparable. The maximum hue change at each image acquisition time step can be calculated for the defined data acquisition time interval. For this purpose, mean wall shear stress values within an operating point-specific wall shear stress interval are evaluated. This data evaluation interval is located around the scaled wall shear stress τ_{ref} at a reference temperature of $T_{ref} = 305$ K, see Table 2. It is set to $\Delta\tau = 0.5$ Pa, see red box in Fig. 6, and is distributed around the optical center of the camera, which corresponds to the geometric center of the measurement insert. The data is scaled according to the reference operating conditions, see Table 1. The results based on the observations of Fig. 6 are presented in Fig. 7. To approximate the resulting values, the curves are fitted. In addition, the change of the hue value relative to the previous time step $\Delta H_i = H_i - H_{i\text{-}1}$ is visualized by the second ordinate on the right and also approximated by curve fitting. The horizontal lines represent values of constant change in averaged hue values. The corresponding numerical values are calculated using Eq. 7 and are listed in Table 2. From the

Table 2: Change in averaged hue value limits for different thresholds, acquisition times according to Eq. 7 and the resulting pre-load times (red markers) from Fig. 7.

Number	ΔH[°]	t_{acq}[s]	ΔH_i[°]	t_{pre}[s]
1	-1	400	0.25	1717
2	-1	300	0.33	1281
3	-2	400	0.50	959
4	-2	300	0.66	787

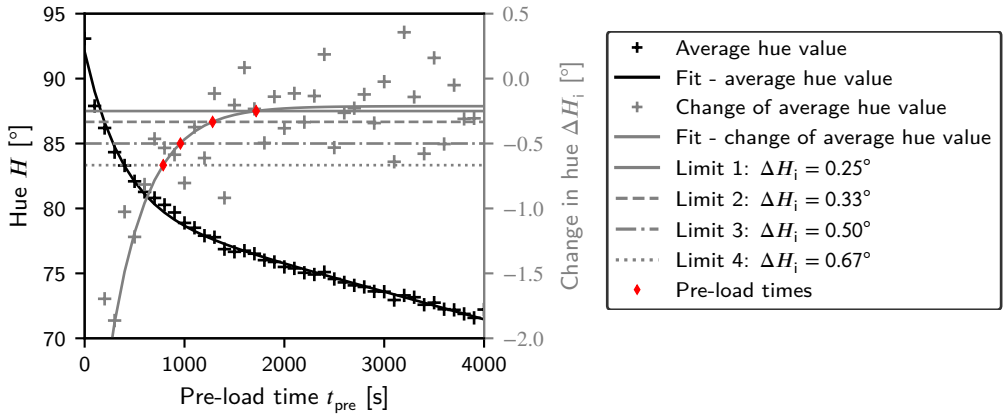

Figure 7: Fitted averaged hue values (left ordinate) and change in averaged hue value ΔH_i (right ordinate) for pre-load times from 0...4 000 s with data acquired every 100 s. The red markers are located at the assumed intersections of the calculated limits ΔH_i and the pre-load times t_{pre} and represent the derived liquid crystal coating pre-load times for the different change in averaged hue values.

numerical values, it can be seen that with a smaller change in hue, e. g. see number 1 of Table 2, the pre-load time increases strongly. In this way, however, it is possible to increase the accuracy during a measurement. Using these derived time constraints, a physical wall shear stress vector field can be calculated. Measurements that consider the derived measurement recommendations and measurements that do not are compared in Fig. 8. For the wall shear stress distribution calculated without considering the pre-load time, a distinct plateau is observed, see range 4...30.2 mm in x-direction in Fig. 8c, black curve. The non-physical increase in wall shear stress at 4 millimeter is due to the transition between flat plate and measurement insert, where small reflections occur. A stronger fluctuation in wall shear stress is also visible between 108.8...135 mm, see Fig. 8c. In Fig. 8a and Fig. 8b, this is indicated by a blue stripe in lateral direction and due to a reflection of the test section on the liquid crystal coating. The same is visible at the transition from the measurement insert to the flat plate, also in the range 108.8...135 mm, see Fig. 8c, where a non-physical decrease of the wall shear stress occurs. The plateau in Fig. 8a is not observed when the pre-load time is considered. When considering the wall shear stress direction, the effect of the pre-load time is particularly noticeable. Without considering the time bias, a clear drift to the right can be observed. However, it is known from the probe measurements that the flow is straight in the direction of the azimuth angle 0°. This drift can be explained by the decreasing hue over time, i.e., from azimuthal position to azimuthal position. In step **III**, see Fig. 5, this leads to a different calculated wall shear stress direction ϕ_τ, whereas the direction of wall shear stress in Fig. 8b corresponds to the intended one, see Melekidis et al. [15].

5.0 GUIDELINES FOR LIQUID CRYSTAL MEASUREMENTS

Quantification of wall shear stress distributions and their directions is challenging, since these quantities cannot be measured directly, but have to be determined by calibration. Liquid crystal diagnostics can provide data with high resolution and low error, provided that the relevant influencing parameters are known and the calibration is performed correctly. Errors may arise from the flow, the acquisition system, and data processing as well as during data acquisition where various effects lead to partly undesired changes in the liquid crystal color signal.

Literature research produced several limitations regarding the applicability and use of liquid crystal diagnostics. Consequently, investigations were carried out to overcome these limitations. A total of three effects were identified, two of which are temperature-related and referred to as (FMR) and (LCR-II) and one of which is due to the thixotropic behavior of the liquid crystals and referred to as (LCR-I). To the authors' knowledge, at least one of the effects found in liquid crystal mixtures for wall shear stress measurements, namely, (LCR-II), is not described at all in literature. The effect due to thixotropy is insufficiently described only. The investigations conducted suggest that all effects have an impact on the liquid crystal color signal and, hence, on the wall shear stress magnitude and its direction. Therefore, appropriate approaches were developed to account for these effects, in both data acquisition and data analysis.

For considering (FMR), the wall shear stress is scaled using a general gas dynamic approach. It is assumed that the density change is negligible. This assumption is valid for the investigated temperature range. The error resulting from this assumption is calculated to be $\approx 4\,\%$. The effect (LCR-II) can be investigated and accounted

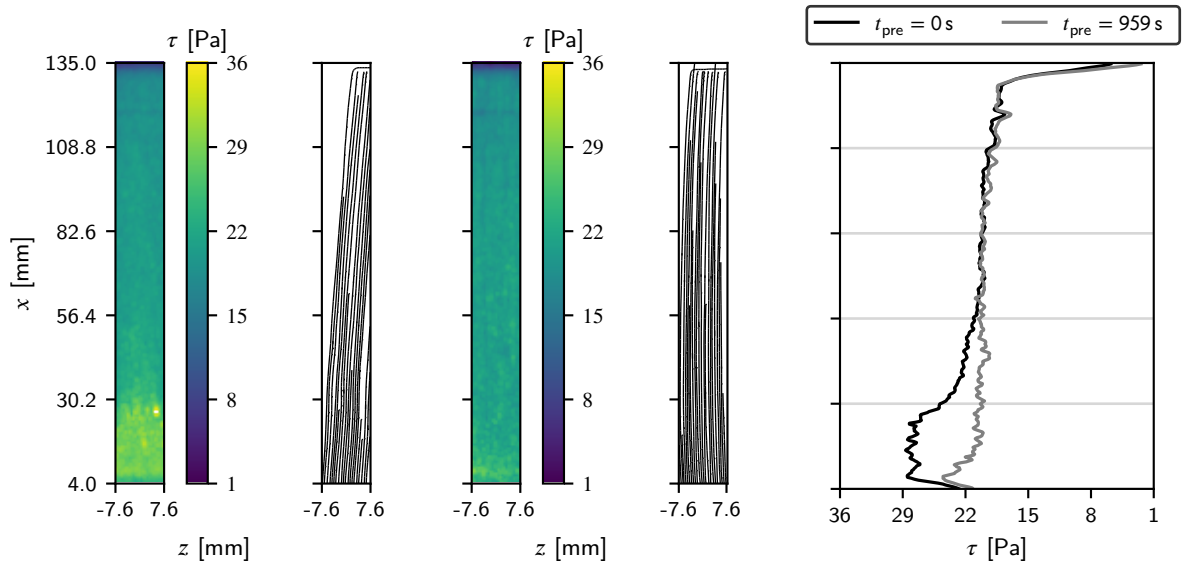

(a) Without consideration of recommendations, after a pre-load time $t_{pre} = 0\,s$

(b) With the recommendations being considered, after a pre-load time $t_{pre} = 959\,s$

(c) Laterally averaged wall shear stress characteristic

Figure 8: Flow field distributions and their directions in cropped and geometrically transformed liquid crystal images obtained from five recordings at different circumferential viewing angles for a fixed above-plane viewing angle of $\alpha_c = 25°$ and an approaching flow from bottom to top, without and with the calculated time constraints being considered.

for by controlled heating of a liquid crystal coating. The change in hue as a function of temperature can then be used to correct the liquid crystal color signal. For the last effect (LCR-I), the developed wall shear stress scaling approach is needed. Using this approach, it is possible to derive time parameters during which the liquid crystal signal is quasi-stationary. The time constraint derived from measurements, namely, the pre-load time of the liquid crystal coating amounts to $t_{pre} = 1\,281\,s$ for a desired recording time of $t_{acq} = 300\,s$ and a tolerable error of $\Delta H = 1°$ for the hue change. This error can be further reduced by reducing the tolerable change in hue, for example. Application of the derived measures shows that the flow field determined by means of liquid crystal diagnostics only agrees with the flow field determined by probe measurements when the time parameters are observed. In particular, the pre-load time is significant for the wall shear stress. Furthermore, a physically lateral averaged wall shear stress characteristic is obtained. From the investigations carried out, the following recommendations and statements are derived for liquid crystal measurements and data processing:

- Although the liquid crystal mixture used is described as shear-sensitive and temperature-insensitive, it is observed to be sensitive to temperature in the range from 293...310 K.
- Liquid crystal data acquisition should be performed under identical boundary conditions, also for the creation of a calibration curve.
- To overcome (LCR-I), the derived time constraints should be considered, i. e. a liquid crystal coating pre-load time and a data acquisition time interval, especially when recording with a single camera.
- To overcome (LCR-II), a preliminary test should be performed to determine the change in hue value due to a temperature change and the calculated hue value should be corrected accordingly.
- To overcome (FMR), the wall shear stress data required to make liquid crystal data comparable at different temperatures, if Mach similarity cannot be achieved while maintaining Reynolds similarity should be scaled.

If the above recommendations are taken into account, reliable and physical data can be obtained with a single commercially available consumer camera.

ACKNOWLEDGEMENT

The authors wish to thank Anna Keim, Oliver Rousseau and Pascal Nguyen for supporting the data acquisition activities at the Institute of Thermal Turbomachinery at KIT. Furthermore, the authors thank the reviewers for their valuable comments, which led to improvements in the manuscript. The responsibility of the content lies solely with the authors.

APPENDIX A: General Settings for Data Acquisition

Table A1: Liquid crystals, illumination, camera boundaries, and operation settings during measurement.

Quantity	Value
Liquid crystal mixture (LC)	BCN/192 [19]
Liquid crystal mixture ratio	1:9 (LC:Acetone) in volume
Measured coating thickness	9 µm ± 4 µm
Illumination source	ILA 5150 LPS v3 (white LED)
Illumination collimation	Telecentric Backlight Illuminator (138 mm)
Light guide	Lumatec Liquid Light Guide (Series 380)
Camera model	Nikon D7200
Lens	Nikon LENS Series E 50 mm k/1.8
Aperture value k	8
Integration time t	0.5 s
ISO value	100
Resolution of acquired image	6 000 px × 4 000 px
Color temperature of white balance	6 250 K
Circumferential viewing angle (azimuthal) ϕ_c	−90°, −45°, 0°, 45° and 90°
Above-plane viewing angle (polar) α_c	25°
Size of region of evaluation	441 px × 51 px
Physical length of region of evaluation	0...131 mm

References

[1] Roach, P. E. 1987. The generation of nearly isotropic turbulence by means of grids. *International journal of heat and fluid flow* 8.2. Pages 82–92

[2] Reda, D. C. and Muratore, J. J. 1994. "A new technique for the measurement of surface shear stress vectors using liquid crystal coatings". In: *32nd Aerospace Sciences Meeting and Exhibit*. Reston, Virigina. DOI: 10.2514/6.1994-729

[3] Reda, D. C., Muratore, J. J., and Heineck, J. T. 1994. Time and flow-direction responses of shear-stress-sensitive liquid crystal coatings. *Journal of American Institute of Aeronautics and Astronautics* 32.4. Pages 693–700. DOI: 10.2514/3.12047

[4] Fujisawa, N., Aoyama, A., and Kosaka, S. 2003. Measurement of shear-stress distribution over a surface by liquid-crystal coating. *Measurement Science and Technology* 14.9. Pages 1655–1661. DOI: 10.1088/0957-0233/14/9/317

[5] Zhao, J., Scholz, P., and Gu, L.-X. 2012. Measurement of surface shear stress vector distribution using shear-sensitive liquid crystal coatings. *Acta Mechanica Sinica* 28.5. Pages 1261–1270. DOI: 10.1007/s10409-012-0144-1

[6] Zhao, J. 2019. Investigation on wall shear stress measurement in supersonic flows with shock waves using shear-sensitive liquid crystal coating. *Aerospace Science and Technology* 85. Pages 453–463. DOI: 10.1016/j.ast.2018.12.034

[7] Zhao, J., Scholz, P., and Gu, L. 2011a. Color change characteristics of two shear-sensitive liquid crystal mixtures (BCN/192, BN/R50C) and their application in surface shear stress measurements. *Chinese Science Bulletin* 56.27. Pages 2897–2905. DOI: 10.1007/s11434-011-4673-y

[8] Zhao, J., Scholz, P., and Gu, L. 2011b. Windtunnel studies of surface shear stress vector distribution measurement using shear sensitive liquid crystal coatings. *Science China Technological Sciences* 54.10. Pages 2730–2734. DOI: 10.1007/s11431-011-4455-4

[9] Zhao, J. 2018. Measurement of Wall Shear Stress in High Speed Air Flow Using Shear-Sensitive Liquid Crystal Coating. *Sensors* 18.5. DOI: 10.3390/s18051605

[10] Anderson, M. R. and Baughn, J. W. 2004. Hysteresis in liquid crystal thermography. *Journal of Heat Transfer* 126.3. Pages 339–346. DOI: 10.1115/1.1738425

[11] Melekidis, S., Elfner, M. R., and Bauer, H.-J. 2022. Towards Quantitative Wall Shear Stress Measurements: A Comparative Study on the Impact of RGB-to-Hue Conversion Algorithms on Liquid Crystal Diagnostics. *Measurement Science and Technology*. DOI: 10.1088/1361-6501/ac8f63

[12] Bonnett, P. 1989. Application of Liquid Crystals in Aerodynamic Testing. Dissertation. University of Oxford

[13] Reda, D. C., Wilder, M. C., Farina, D. J., et al. 1997. New Methodology for the Measurement of Surface Shear Stress Vector Distributions. *Journal of American Institute of Aeronautics and Astronautics* 35.4. Pages 608–614. DOI: 10.2514/2.165

[14] Bajón, J., Cattoen, M., and Kim, S. D. 1985. Techniques de transformations colorimetriques en temps reel implantees sur un module de vision pour la robotique. *Actes de la conference MICAD*. Pages 76–86

[15] Melekidis, S., Elfner, M. R., and Bauer, H.-J. 2020. "Towards Quantitative Wall Shear Stress Measurements: Calibration of Liquid Crystals". In: *Proceedings of the ASME Turbo Expo: Turbomachinery Technical Conference and Exposition - 2021*. Vol. 5: Controls, Diagnostics, and Instrumentation; Cycle Innovations; Cycle Innovations: Energy Storage. Turbo Expo: Power for Land, Sea, and Air, V005T05A005. DOI: 10.1115/GT2020-14381

[16] Schlichting, H., Gersten, K., and Krause, E. 2006. Grenzschicht-Theorie: Mit 22 Tabellen. 10th ed. Berlin, Heidelberg. DOI: 10.1007/3-540-32985-4

[17] Leslie, F. M. 1969. Continuum Theory of Cholesteric Liquid Crystals. *Molecular Crystals* 7.1. Pages 407–431. DOI: 10.1080/15421406908084887

[18] White, F. M. 1991. Viscous fluid flow. 2nd ed. McGraw-Hill series in mechanical engineering. New York. ISBN 0-07-069712-4

[19] LCRHallcrest. 2014. Handbook of Thermochromic Liquid Crystal Technology. https://cupdf.com/document/lcr-hallcrest-handbook-of-liquid-crystal-technology-rt006-rev01-usa.html?page=2